Stacking Catalog Sources in WMAP Data

Kasey W. Schultz, Kevin M. Huffenberger

University of Miami

DEPARTMENT OF PHYSICS

ABSTRACT

Following Sawangwit & Shanks (2010a), we stack WMAP 7-year temperature data around extragalactic point sources to probe deviations in the source profiles from the Jupiter-modeled WMAP beams. Like them, for WMAP catalog sources we find that the stacked source profiles are broader than the WMAP model beam. Subtracting a galactic foreground model changes the stacked profiles, particularly at Q-band, but even after subtraction, the profiles are significantly wider than the WMAP models in the Q-, V-, and W-bands. However, we find that the profiles of NVSS-selected sources are consistent with the WMAP beam models, in conflict with the finding of Sawangwit & Shanks (2010a), and we attribute their result to galactic foreground. Our NVSS profiles provide strong evidence that the broad profiles around WMAP sources are caused by selection bias at the faint end of the WMAP catalog, where faint sources aligned with a positive CMB fluctuation may be boosted above the WMAP catalog threshold. With parametric beam models, we explore other explanations for the broad profiles, including source spectral energy distribution and positional uncertainty, but discard them as unlikely.

DATA

Data:
Our analysis uses the WMAP 7-year point source catalog and temperature maps. Our final analysis uses the foreground-reduced maps provided by the WMAP team. We also use the NRAO VLA Sky Survey point source catalog, taking bright sources with flux density greater than 2 Jy at 1.4 GHz.

Masking:
To mask residual galactic foreground, we use the WMAP 7-year temperature analysis mask combined with the point source catalog mask (inverted to retain sources). To eliminate sources in foreground dominated regions we smooth with a 2º FWHM Gaussian and apply a 90% threshold to obtain the mask shown in Figure 1.

Neighbor Exclusion:
We use pixels out to θ_{max} = 1º from the source positions, so we must exclude all sources separated by less than $2\theta_{max}$ to avoid overlap. After these cuts, 365 WMAP-selected sources and 370 NVSS-selected sources remain.

WMAP & NVSS STACKING

Why stack?:
Observing the sky convolves it with telescope's beam pattern, hence bright point-like objects are smoothed to resemble the beam. Therefore, stacking extragalactic point sources is a means to recover the beam pattern.

A challenge:
Sawangwit & Shanks (2010a) stacked WMAP 5-year data around WMAP source catalog positions, finding stacked profiles much broader than the WMAP beam modeled from Jupiter measurements. Noting the sensitivity of WMAP's power spectrum measurement to the beam reconstruction, they present this as a challenge to the ΛCDM model.

Procedure:
We stack sources by defining angular annuli about their catalog position, then average pixels enclosed by the annuli.
For WMAP-selected sources we see broad profiles similar to Sawangwit & Shanks (2010a), and like them, we note that faint sources have broader profiles than bright ones. In conflict with their result, for NVSS-selected sources, we find that the profiles resemble the WMAP beam models, unless we neglect to remove the foreground model.

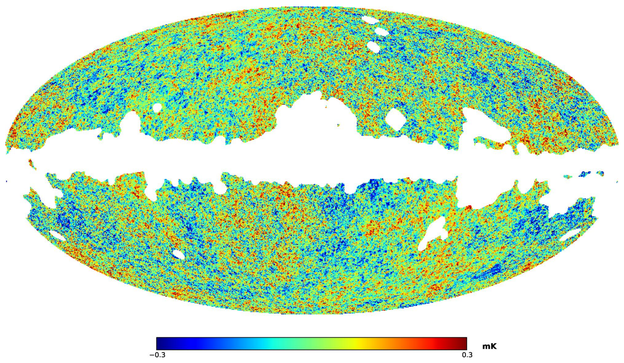

Figure 1: WMAP foreground-reduced V1 map with mask applied.

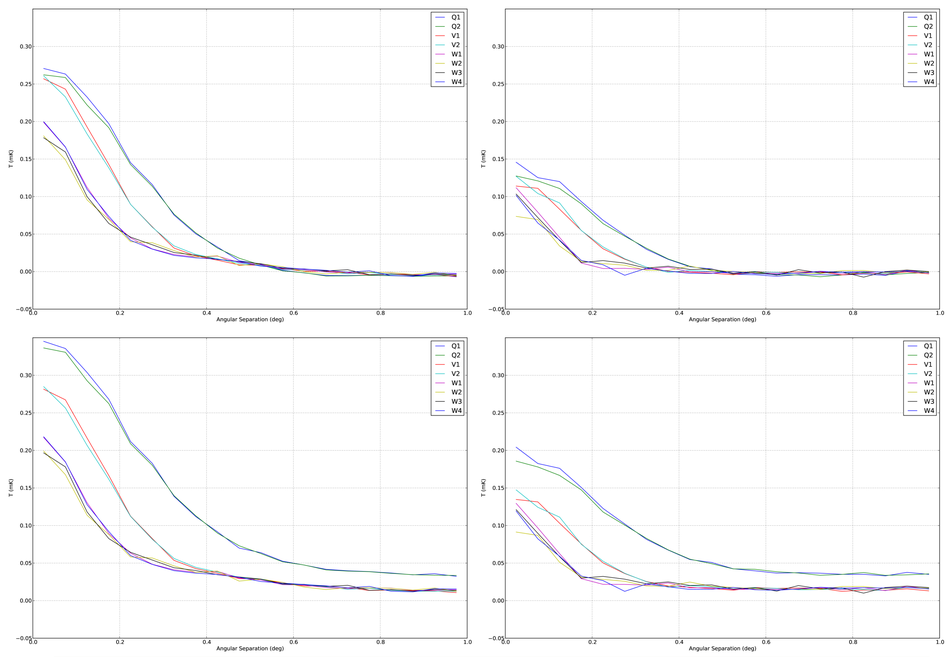

Figures 2 & 3 (top): Stacked profiles for WMAP catalog (left) and NVSS catalog (right) on foreground-reduced maps.
Figures 4 & 5 (bottom): Same profiles for maps including foreground emission, note the vertical offset.

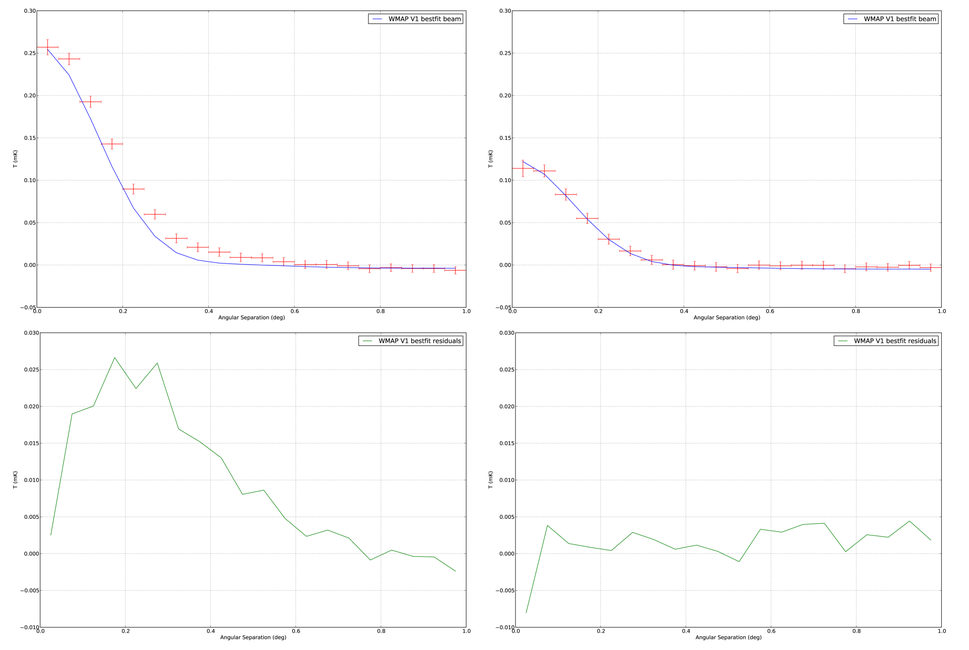

Figures 9 &10 (top): Amplitude/offset best-fit for WMAP (left) and NVSS (right) catalog sources. The WMAP profile fits poorly.
Figure 11 & 12 (bottom): Residuals of above fits. Note that NVSS residuals are flat, WMAP residuals show definite structure.

PROFILE FITTING

We minimize χ^2 comparing model profiles to the stacked data using two contributions to the covariance of profile bins: detector noise and background CMB fluctuations (assuming that sources are uncorrelated with CMB). We compute the noise covariance analytically and the CMB covariance with ΛCDM simulations. Figures 6-8 show the covariance matrices. The detector noise covariance is diagonal, but the CMB fluctuations are strongly correlated between profile bins.

To explore the broad profiles, we designed increasingly complicated profile models based on the Jupiter-modeled WMAP beam. The profiles for NVSS-selected sources are well-fit by the simplest model. No model adequately explains the profiles for WMAP-selected sources.

Amplitude/offset model:
The simplest model has a temperature amplitude factor and constant temperature offset. This should fit the data well if Jupiter-modeled beams are reliable. The best-fit model and residuals are shown in Figures 9-12 for WMAP- and NVSS-selected sources. This model is a bad fit for the WMAP sources (for V1, χ^2 = 89.6, 18 d.o.f., $P(>\chi^2) = 1.8\times10^{-11}$) but a good fit for NVSS sources (for V1, χ^2 = 19.0, 18 d.o.f., $P(>\chi^2)$ = 0.39). There are similar results for all DAs in Q, V, and W bands.

Angular scaling:
This model adds a parameter that scales θ, which can check the bandpass effective frequency for sources, which potentially can broaden the profile. For WMAP sources, the χ^2 of this fitting in each band was also poor, and the best-fit effective frequency was unrealistically low given the measured SEDs of WMAP sources.

Positional uncertainty:
In this model, instead of an angular scaling, we convolve the beam with a Gaussian, which probes uncertainty in WMAP catalog positions. For WMAP sources, again the χ^2 of this fitting was poor, which returned a best-fit positional uncertainty that was far too big.

Flux-dependent positional uncertainty:
If the width of the Gaussian is allowed to vary as a power law with source flux density, as if faint sources had greater positional uncertainty than bright ones, we can obtain good fits for WMAP source profiles. However, the required power law index is inconsistent between the bands, making this explanation unlikely.

COMMON FLUCTUATIONS

The covariance for profile fitting assumed the sources were independent from the CMB. For NVSS sources selected at 1.4 GHz, where the CMB is weak, this is a good assumption, and we find agreement with the Jupiter-modeled beam. For WMAP selected sources, the stacked profiles are wide, and this assumption appears to break down.

The residuals to the fit in Figures 11 and 12 suggest that the source profile may sit atop another temperature fluctuation; the similarity in the outer parts of the profiles at different frequency bands in Figure 4 suggest that the CMB is the source of that fluctuation.

The underlying fluctuation can estimated by averaging the residuals from the individual amplitude/offset fits. We can improve this estimate by combining the data from multiple DAs and solve a linear system for the amplitude and residual fluctuations in one step, employing the proper noise weighting for each profile bin. The resulting estimates are shown in Figure 13.

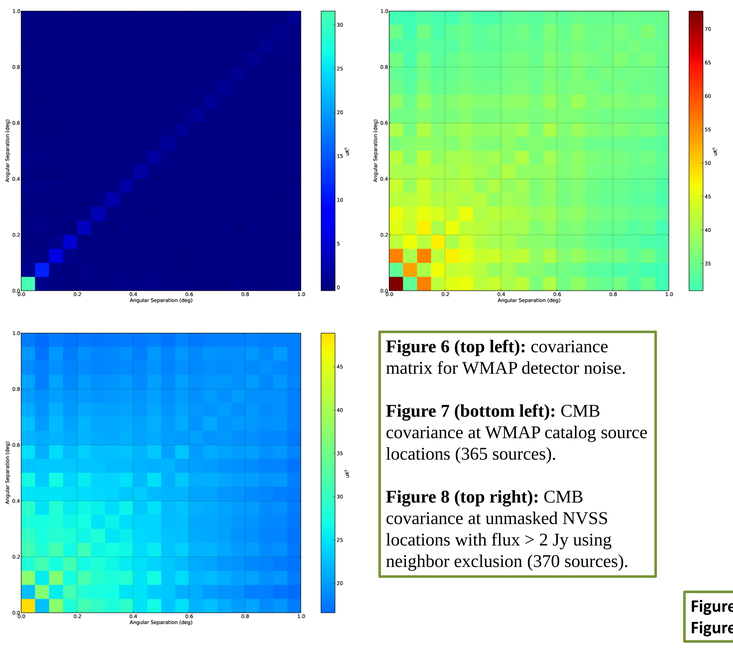

Figure 6 (top left): covariance matrix for WMAP detector noise.

Figure 7 (bottom left): CMB covariance at WMAP catalog source locations (365 sources).

Figure 8 (top right): CMB covariance at unmasked NVSS locations with flux > 2 Jy using neighbor exclusion (370 sources).

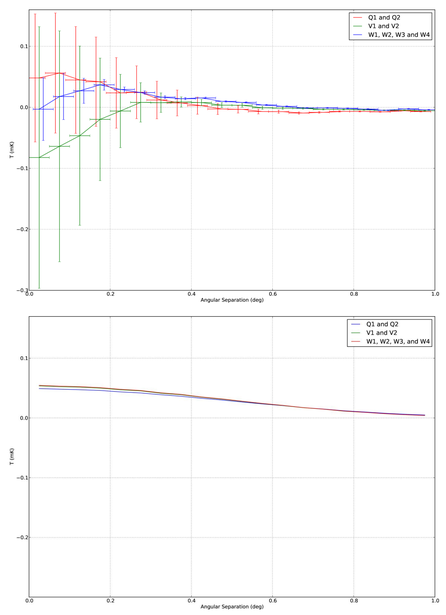

Figure 13 (top): Common fluctuation estimates for WMAP profiles.
Figure 14 (bottom): Simulation of average CMB fluctuation for boosted sources.

SELECTION BIAS

If WMAP catalog sources are preferentially selected to lie on positive CMB fluctuations, those fluctuations, which have significant power on scales larger than the beam, can broaden the stacked source profiles.

This is reasonable, because for sources near the catalog threshold, sources that have their measured flux boosted by CMB fluctuations will tend to be included in the catalog, while those that have their measured flux suppressed will tend to be excluded. Since this effect is most significant near the catalog threshold, it explains why faint WMAP sources show broader profiles than bright ones.

As a first step to examine this effect, we assess the average impact on the source profile for those K-band selected sources that receive a positive boost. Our prescription follows:

* Simulate a CMB-only map with K-band noise.
* Filter it with a filter optimized to find point sources.
* At random positions, determine whether the filtered map exceeds zero at that point (positive indicates a flux boost).
* For boosted sources, stack the unfiltered CMB-only simulation around that position.

Figure 14 shows this estimate for an average over 1000 maps with 100 prospective sources per map. Although similar in size and shape to the fluctuation estimated from the data, this does not account for flux-suppressed sources that remain in the catalog, which requires a more detailed estimate.

CONCLUSIONS

We stack WMAP temperature data around WMAP and NVSS catalog sources. For WMAP sources, we find broad profiles similar to Sawangwit and Shanks (2010a), but for NVSS-selected sources, the profiles are consistent with the WMAP beams. Removal of galactic foregrounds is required. Several parametric models fail to account for the WMAP profiles.

The most likely explanation is that the broad profiles are caused by residual CMB fluctuations. These underlying fluctuations are preferentially positive because of a bias in the WMAP catalog selection. We plan a complete 5-band mock-WMAP source catalog simulation to examine the selection effect in more detail.

Acknowledgements:
This work was supported by NASA's Florida Space Grant Consortium, Beyond the Book program from the University of Miami College of Arts and Sciences, and NASA-JPL subcontract 1363745.

REFERENCES

1) Giannantonio T. et al., 2010, Astronomy and Geophysics, 51, 050000
2) Jarosik N. et al., 2007, ApJS, 170, 263
3) Nolta M. R., 2009, ApJS, 180, 296
4) Sawangwit U., Shanks T., 2010a, MNRAS, L93+, 2010b, Astronomy and Geophysics, 51, 050000, 2010c, ArXiv e-prints
5) Wright E. L., 2009, ApJS, 180, 283